RESEARCH ARTICLE

THE FASEB JOURNAL

Modulation of transcriptional mineralocorticoid receptor activity by casein kinase 1

Stefanie Ruhs[1,2] | Bruno Griesler[1] | Ralf Huebschmann[1] | Katharina Stroedecke[1] | Nicole Straetz[1] | Christian Ihling[3] | Andrea Sinz[3] | Antonia Masch[4] | Mike Schutkowski[4] | Michael Gekle[1] | Claudia Grossmann[1]

[1]Julius Bernstein Institute of Physiology, Martin Luther University Halle-Wittenberg, Halle (Saale), Germany

[2]Department of Anesthesiology and Surgical Intensive Care, University Hospital Halle (Saale), Halle (Saale), Germany

[3]Department of Pharmaceutical Chemistry & Bioanalytics, Center for Structural Mass Spectrometry, Institute of Pharmacy, Martin Luther University Halle-Wittenberg, Halle (Saale), Germany

[4]Department of Enzymology, Institute of Biochemistry and Biotechnology, Martin Luther University of Halle-Wittenberg, Halle (Saale), Germany

Correspondence
Claudia Grossmann, Julius Bernstein Institute of Physiology, Martin Luther University Halle-Wittenberg, Magdeburger Straße 6, 06112 Halle (Saale), Germany.
Email: claudia.grossmann@medizin.uni-halle.de

Funding information
This study was supported by the Deutsche Forschungsgemeinschaft (DFG): grant GR 3415/1-5 (CG) and RTG 2155 ProMoAge SP11 (CG) as well as the European Section of the Aldosterone Council (ESAC) (SR) and HaPKoM (Graduate School of Medicine, Halle) (BG)

Abstract

The mineralocorticoid receptor (MR) with its ligand aldosterone (aldo) physiologically regulates electrolyte homeostasis and blood pressure but it can also lead to pathophysiological effects in the cardiovascular system. Previous results show that posttranslational modifications (PTM) can influence MR signaling and function. Based on *in silico* and in *vitro data*, casein kinase 1 (CK1) was predicted as a candidate for MR phosphorylation. To gain a deeper mechanistic insight into MR activation, we investigated the influence of CK1 on MR function in HEK cells. Co-immunoprecipitation experiments indicated that the MR is located in a protein–protein complex with CK1α and CK1ε. Reporter gene assays with pharmacological inhibitors and MR constructs demonstrated that especially CK1ε acts as a positive modulator of GRE activity via the C-terminal MR domains CDEF. CK1 enhanced the binding affinity of aldosterone to the MR, facilitated nuclear translocation and DNA interaction of the MR, and led to expression changes of pathophysiologically relevant genes like *Per-1 and Phlda1.* By peptide microarray and site-directed mutagenesis experiments, we identified the highly conserved T800 as a direct CK1 phosphorylation site of the MR, which modulates the nuclear import and genomic activity of the receptor. Direct phosphorylation of the MR was unable to fully account for all of the CK1 effects on MR signaling, suggesting additional phosphorylation of MR co-regulators. By LC/MS/MS, we identified the MR-associated proteins NOLC1 and TCOF1 as candidates for such CK1-regulated co-factors. Overall, we found that CK1 acts as a co-activator of MR GRE activity through direct and indirect phosphorylation, which accelerates cytosolic-nuclear trafficking, facilitates nuclear accumulation and DNA binding of the MR, and increases the expression of pathologically relevant MR-target genes.

Abbreviations: aldo, aldosterone; CK1, casein kinase 1; CK2, casein kinase 2; CREB, cAMP response element-binding protein; CTD, C-terminal domain; DBD, DNA-binding domain; dexa, dexamethasone; ENaC, epithelial Na$^+$ channel; GRE, glucocorticoid response element; LBD, ligand binding domain; MR, mineralocorticoid receptor; NFAT, nuclear factor of activated T-cells; NOLC1, nucleolar and coiled-body phosphoprotein 1; NTD, N-terminal domain; Per-1, period circadian regulator 1; Phlda1, pleckstrin homology-like domain family A member 1; PTM, posttranslational modifications; SEAP, secreted alkaline phosphatase; TCOF1, treacle protein; TMT, tandem mass tag.

1 | INTRODUCTION

The mineralocorticoid receptor (MR) is a ligand-dependent transcription factor that belongs to the nuclear receptor (NR) subfamily 3, which also includes another corticosteroid receptor, the glucocorticoid receptor (GR) and sex hormone receptors like the estrogen, progesterone, and androgen receptor. Besides regulating electrolyte homeostasis and blood pressure, the MR can mediate inflammatory, fibrotic, and hypertrophic processes in the renocardiovascular system.[1–3] Thereby, it is involved in aging-associated disorders and diseases of the cardiovascular system. Upon aldosterone (aldo) binding, the MR translocates HSP90-dependently into the nucleus, binds to transcriptional co-factors, and interacts with target gene promoters.[4] Classical hormone response elements shared by MR and GR are glucocorticoid response elements (GRE). Transcriptional specificity and control by MR are achieved by the coordinated recruitment of co-activators and co-repressors and can be modulated by posttranslational modifications (PTM) (e.g., sumoylation, acetylation, oxidation, ubiquitylation).[3,5] In this context, phosphorylation is an important PTM that regulates the activity of the MR.[2,6–8] For example, phosphorylation of MR-S459 by casein kinase 2 (CK2) leads to increased genomic MR activity.[7] In contrast, cyclin-dependent kinase 5 (CDK5) interacts with the C-terminal ligand-binding domain (LBD) and leads to phosphorylation of S128, S250, and T159, resulting in reduced genomic activity.[9] Shibata et al. showed that phosphorylation at S843 in the LBD prevents aldo binding and activation of MR and thereby regulates the renal response to hyperkalemia and volume depletion.[10] These studies show how the phosphorylation of individual amino acids of MR can affect its functionality.

The ubiquitously expressed serine/threonine-casein kinase 1 (CK1) isoforms are permissive drug targets that play a role in aging-associated neurodegenerative diseases and cancer[11] and are also candidates for phosphorylating and modulating steroid receptors including the MR. CK1 family members are monomeric, constitutively active kinases, consisting of six human isoforms (α, $\gamma1$-$\gamma3$, δ and ε).[12] CK1 recognizes mainly acidic or pre-phosphorylated amino acid residues with the canonical consensus sequence represented by the motif D/E-X-X-(X)-Ser/Thr or pSer/pThr-X-X-(X)-Ser/Thr.[13] CK1 modulates numerous cellular processes, including the circadian rhythm by phosphorylating the central clock genes period circadian protein homolog 1-3 (*Per1-3*).[12–14] *Per-1* is a MR-induced gene that is influenced in its function by CK1δ/ε, leading to fine-tuning of αENaC expression and sodium reabsorption in the kidney.[15,16] Sodium reabsorption modulates volume and blood pressure and ENaC is an important player for MR-induced volume and blood pressure regulation. A perturbed circadian rhythm also facilitates aging, learning disabilities, and cardiovascular diseases. CK1 is also involved in the regulation of nuclear trafficking of different transcription factors. For example, CK1α-induced phosphorylation of NFAT leads to masking of the nuclear localization sequence and prevents import and activity of NFAT.[17] Furthermore, the genomic activity of the estrogen receptor α (ERα), a family member of the MR, is increased CK1δ-dependently by phosphorylation of ERα and the steroid receptor co-activator 3 (SRC-3).[18] Currently, the influence of CK1 isoforms on MR functionality has not been explored. Therefore, we investigated the possible crosstalk between CK1 and MR and analyzed the impact of CK1 isoforms on MR activity. The mechanisms of altered genomic MR activity were studied, including (i) relevant MR domains and DNA response elements, (ii) cytosolic nuclear shuttling of the MR, (iii) altered subcellular distribution of the MR, (iv) MR-DNA interaction, and (v) direct phosphorylation of MR residues versus indirect effects of CK1. Finally, the functional relevance of the MR-CK1 interaction for transcriptional processes was analyzed using the genes *Per-1* and *Phlda1* as marker genes.

2 | MATERIALS AND METHODS

2.1 | Cell culture

HEK cells, from American Type Culture Collection (Rockville, MD), were cultivated in DMEM/Ham's F-12 medium supplemented with 10% fetal calf serum (FCS) at 37°C with 5% CO_2 as described previously and sub-cultivated once a week. After serum-starvation (24 h), cells were treated with vehicle (DMSO 0.1%), aldo, respective CK1 inhibitors, or a combination of aldo and CK1 inhibitors for different time points. The following CK1 inhibitors were used: D4476 (4-[4-(2.3-dihydro-1, 4-benzodioxin-6-yl)-5-(2-pyridinyl)1H-imidazol-2-yl]-b enzamide), PF-670462 (4-[1-Cyclohexyl-4-(4-fluorophe nyl)-1H-imidazol-5-yl]-2-pyrimidinamine dihydrochloride) and PF-4800567 (3-[(3-Chlorophenoxy)methyl]-1-(tetrahydro-2H-pyran-4-yl)-1H-pyrazolo[3,4-d] pyrimidin-4-amine hydrochloride).

The T-Rex System (Thermo Fisher Scientific, Waltham, MA, USA) was used to create a tetracyclin- inducible MR overexpressing HEK cell clone that was cultivated in DMEM medium supplemented with 25 mM glucose, 10% FCS, blasticidin S (Gibco; Thermo Fisher Scientific, Karlsruhe, Germany) and zeocin (Invitrogen, Thermo Fisher Scientific, Karlsruhe, Germany). For the experiments presented, Tet-inducible MR HEK cells were serum-starved for 6 h followed by MR induction with tetracycline (0.25 μg/ml) for 18 h. Tet-induced MR cells were stimulated with vehicle, aldo, D4476 or aldo + D4476 for the indicated time points. EA.hy926 cells (ATCC) were cultivated in DMEM with 2 g/L NaHCO$_3$.

2.2 | Transfection

Transfection of HEK cells was performed with Polyfect reagent (Qiagen, Hilden, Germany), according to the manufacturer's instructions. HEK cells were transfected with the MR expression vector pEGFP-C1-hMR (kind gift of N. Farman, Paris), with pEGFP-hMR[CDEF] Ref. [19]: pEGFP-C1 (Clontech), the GR expression vector pEGFP-C1-hGR or pcDNA3.1-His-LacZ (control vector, Invitrogen).

2.3 | Quantitative PCR

Total RNA was isolated using the InviTrap Spin Tissue RNA Mini Kit (STRATEC Molecular GmbH, Berlin, Germany) with an additional DNase I digestion. RNA was subjected to reverse transcription with SuperScript II reverse transcriptase (Thermo Fisher Scientific, Waltham, MA, USA) and random primers. Real time PCR (7900HT Fast Real-time PCR system, Applied Biosystems, *via* Thermo Fisher Scientific, Karlsruhe, Germany) was performed utilizing Platinum SYBER Green Quantitative PCR Supermix (Thermo Fisher Scientific, Waltham, MA, USA). Fold changes in expression levels were calculated by the 2ΔΔCq method, using the 18S rRNA signal for normalization. Table S1 shows the utilized primers.

2.4 | Droplet digital PCR

For analyzing the absolute RNA amount of each of the CK1 isoforms droplet digital PCR™ was conducted using the QX200 system (Biorad, Munich, Germany). cDNA was prepared as described above and used in droplet digital PCR (ddPCR) under the following conditions: 95°C for 10 min followed by 40 cycles of 95°C for 30 s and 60°C for 1 min, with ramp rates of 2°C·s^{-1}. Table S1 shows utilized primers.

2.5 | Protein determination

Protein content was determined using the bicinchoninic acid assay (Thermo Scientific, Schwerte, Germany) with bovine serum albumin as standard.

2.6 | Coimmunoprecipitation

Cells were transfected with pEGFP-C1 or pEGFP-hMR and incubated with vehicle or aldo (10 nM) for 1 h. Coimmunoprecipitation (CoIP) experiments were performed with anti-GFP-coupled magnetic beads and μ columns (Miltenyi, Bergisch Gladbach, Germany) as recommended by the manufacturer followed by Western blot analysis as described earlier.[7]

2.7 | Western blot

Western blot was performed according to standard protocol. Cells were lysed with RIPA buffer (in mM: NaCl 150, Tris (base) 10, pH 7.4, Na-orthovanadate 1, EDTA 1, Triton X-100 1%, Nonidet P-40 1%, SDS 0.1%, Na-deoxycholate 1%, protease inhibitor cocktail). 25–50 μg protein/lane was separated by 8%–12% SDS-PAGE, transferred to nitrocellulose membrane, and incubated with the following primary antibodies: anti-rMR1-18 1D5 (DSHB, University of Iowa, USA), anti-HSP90 (Cell Signaling, USA), anti-GAPDH (Cell Signaling, USA), anti-CK1α (abcam, Berlin, Germany), anti-CK1δ (Cell Signaling, USA), anti-CK1ε (R&D systems, Minneapolis, Canada), and anti-β-actin (Cell Signaling, USA). The effective binding of the primary antibody (anti-MR, anti CK1ε) was visualized using horseradish peroxidase (HRP)-conjugated IgG secondary antibodies (Cell signaling, USA) and the Clarity™ Western ECL substrate (Biorad, Munich, Germany) with the Molecular Imager ChemiDoc XRS System (Biorad, Munich, Germany). Densitometry analyses were performed with Quantity One® (Biorad, Munich, Germany). The effective binding of the primary antibody (anti-CK1α, anti-CK1δ, anti-HSP90, anti-β actin, anti-GAPDH) was visualized using fluorescence dye-conjugated (IRdye 680RD or IRdye 800CW) secondary antibodies (Li-cor, Bad Homburg, Germany) with the Odyssey® Imaging system, version 3.0 (Li-cor, Bad Homburg, Germany). Quantitative analysis was performed with the Image Studio Lite Version 5.2 (Li-cor, Bad Homburg, Germany).

2.8 | Secreted alkaline phosphatase (SEAP) reporter gene assay

Reporter gene assays with secretory alkaline phosphatase as a reporter were performed by using the Mercury Pathway Profiling reporter gene assay system (Clontech) as described previously.[19] SEAP activity was measured by fluorescence measurements with the AttoPhos System (Promega, Mannheim, Germany). Beta-galactosidase encoded by pcDNA3.1Hislacz (Invitrogen, Darmstadt, Germany) was co-transfected as an internal control. The beta-galactosidase activity was measured by a colorimetric assay with ortho-nitrophenyl-β-galactoside as substrate and photometric measurement at 405 nm. The SEAP activity was normalized to the transfection control β-galactosidase or the protein content determined by the BCA assay (see also supplemental methods).

2.9 | Time-lapse experiments

To determine cytosolic-nuclear MR shuttling during different treatment conditions, we performed time-lapse experiments using a digital BZ-8000 fluorescence microscope with an integrated camera and corresponding software from Keyence (Osaka, Japan) with an incubation chamber preheated to 37°C. HEK cells were seeded in cell culture μ-dishes (ibidi, Martinsried, Germany), transfected with pEGFP-hMR or pEGFP-MR mutants for 6 h in medium without serum or supplements. During the experiment, the cells were incubated in Hepes buffer (in mM: NaCl 122.5, KCl 5.4, MgCl·6H$_2$O 0.8, CaCl$_2$·2H$_2$O 1.2, NaH$_2$PO$_4$·H$_2$O 1, Hepes 10, pH 7.4, at 37°C) containing glucose (5.5 mM) and incubated with vehicle, aldo (10 nM), D4476 (10 μM), or D4476 + aldo. Basal EGFP fluorescence was subtracted and maximal EGFP fluorescence of the cell was normalized to 1. The normalized fluorescence intensity was plotted over time and the half life time and the maximum translocation velocity index, which corresponds to the slope of the curve, were determined using Sigma Plot software.

2.10 | Electrophoretic mobility shift assays (EMSAs)

Electrophoretic mobility shift assays were performed with the LightShift Chemiluminescence EMSA Kit (Thermo Fisher Scientific, Waltham, MA, USA). HEK cells were transiently transfected with the EGFP-MR (0.035 ng/cm²) for 24 h followed by the generation of cell lysates using non-denaturing RIPA buffer (mM: Tris (base) 50, pH7.4.;

NaCl 150, ETDA 1, Nonidet P-40 1%, Na-deoxycholate 0.25%, protease inhibitor cocktail). Cell lysates were then incubated for 1 h on ice with vehicle, aldo (10 nM), D4476 (10 μM) or aldo + D4476. Biotinylated DNA probes (GRE) were produced by oligo hybridization: (GRE sense: CTAGCGGTACATTTTGTTCTAGAAC; GRE antisense: GTTCTAGAACAAAATGTACCGCTAG). Binding reactions were carried out for 30 min at room temperature in the presence of 10 mM Tris, 50 mM KCl, 5 mM MgCl$_2$, 1 mM DTT, 5% glycerol, and 1 μg/μl poly (dI-dC). Biotinylated GRE probe was used in a concentration of 2ng per reaction and incubated with 12 μg EGFP-MR overexpressing cell lysate. Electrophoresis of the DNA–protein complexes was carried out with a 5% to 10% non-denaturing gradient polyacrylamide gel. Samples were transferred to a nylon membrane at 300 mA for 37 min and cross-linked on the membrane at 120 mJ/cm² for 1 min. For visualization, the Chemiluminescent Nucleic Acid Detection Module was applied (Thermo Fisher Scientific, Waltham, MA, USA) with extended washing steps.

2.11 | Site-directed mutagenesis

The EGFP-MR mutants T800A, S936A were prepared using the MR expression vector pEGFP-C1-hMR and the QuikChange II XL Site-Directed Mutagenesis Kit (Agilent Technologies, Santa Clara, USA) as recommended by the manufacturer. Cloning results were confirmed by sequencing (Microsynth Seqlab, Göttingen).

2.12 | Peptide microarrays

Peptide microarrays were performed as described earlier.[7] In general, the peptide microarrays were produced by JPT Peptide Technologies GmbH (Berlin, Germany). Every MR peptide was composed of 15 aa with 12 aa overlap resulting in 341 peptides. Each peptide was spotted three times in triplicates resulting in a ninefold presentation of each individual peptide. Microarrays were incubated with recombinant CK1 (500 U) (New England Biolabs, USA) in a kinase buffer (in mM: Tris-HCl 20, pH 7.5, MgCl2 10, KCl 50, ATP 0.25 μM, 0.36 MBq γ-33P-ATP) for 2 h at 25°C in a humid chamber as described by Ref. [7]. After rigorous washing, the incorporated radioactivity was detected by 26 h lasting exposure of the peptide microarrays to imaging plates (Fuji BAS-MS, Fuji Photo Film Co.) followed by readout with a FLA 3000 phosphor imager (Fuji). Control experiments with radioisotopically labeled ATP in buffer without kinase did not yield any signal after phosphor imaging. The peptide microarrays were analyzed according to the described criteria[7]: (i) nine spots of the peptide on

the peptide microarray had to be phosphorylated; (ii) clear signal intensity; (iii) a phosphorylation trend i.e., serine/threonine of interest was phosphorylated in more than one overlapping peptide.

2.13 | Protein Isolation and TMT labeling

HEK cells were transiently transfected with EGFP as a negative control or with EGFP-MR in four separate experiments. After 24 h serum starvation and DMSO treatment (24 h) an EGFP pulldown was performed utilizing anti-GFP-coupled magnetic beads and μ columns (Miltenyi, Bergisch Gladbach, Germany) as recommended by the manufacturer. The Co-IP eluates were precipitated with a fourfold volume of ice-cold acetone and incubated overnight at −80°C. The further preparation of the samples was carried out as described in the supplemental methods and by Ihling et al.[20]

2.14 | Liquid chromatography-mass spectrometry/mass spectrometry (LC/MS/MS analysis)

A total of 2 μg protein was injected on an Ultimate 3000 RSLC nano-HPLC system (Thermo Fisher Scientific, Bremen, Germany) and separated using reversed-phase C18 columns (trapping column: Acclaim PepMap C18, 100 μm × 20 mm, 3 μm, 100 Å, separation column: EASY-Spray column, Acclaim PepMap C18, 75 μm × 500 mm, 2 μm, 100 Å, Thermo Fisher Scientific, Bremen, Germany). After washing the peptides on the trapping column for 15 min with 0.1% TFA at a flow rate of 20 μl/min, peptides were eluted and separated using 270-min gradients from 1% to 35% solvent B (solvent A: 0.1% formic acid in water, solvent B: 0.08% formic acid in acetonitrile) at a flow rate of 270 nl/min. The nano-HPLC system was directly coupled to the nano-ESI source (EASY-Spray source, Thermo Fisher Scientific, Bremen, Germany) of an Orbitrap Fusion Tribrid mass spectrometer (Thermo Fisher Scientific, Bremen, Germany). Samples were analyzed with a combined CID/HCD (collision-induced dissociation/higher-energy collision-induced dissociation) MS/MS strategy for peptide identification and reporter ion quantification. FTMS survey scans were acquired over the m/z range 300–1500 every 5 s ($R = 120\,000$ at m/z 200, AGC (automated gain control) target value 4×10^5, max. injection time 50 ms). CID fragment ion spectra of the most abundant signals of the survey scans were acquired in the linear ion trap (LTQ; quadrupole isolation window 2 Th, 35% normalized collision energy (NCE), AGC target 1×10^4, max. injection time 100 ms). The same precursor

ions were selected for stepped HCD experiments (quadrupole isolation window 1.3 Th, 30, 35, 40% NCE, AGC target 5×10^4, max. injection time 150 ms); HCD fragment ion spectra were acquired in the orbitrap analyzer ($R = 60\,000$ at m/z 200) to resolve reporter ions with the same nominal mass. Dynamic exclusion was enabled (exclusion time 45 s). MS data analysis was performed as described in the supplemental methods.

2.15 | Statistics

Data are presented as mean ± standard error mean (SEM). The computer program used to create the figures was Sigma Plot 12. Significance of difference was tested by paired or unpaired Student's t test with $p \leq .05$ considered statistically significant. N represents the number of individual experiments and n is the number of wells or culture dishes investigated per experiment.

3 | RESULTS

3.1 | CK1α and ε isoforms interact with the MR in a protein-protein complex

In silico analysis predicted CK1 and CK2 as candidates for direct MR phosphorylation. CK2 was already investigated previously.[7] To explore the impact of CK1, we analyzed the mRNA expression of the different CK1 isoforms in HEK cells by ddPCR and found CK1α and CK1ε to be abundantly expressed in contrast to the other isoforms (Figure 1A). CK1α and CK1ε could be specifically co-immunoprecipitated with EGFP-MR under basal as well as aldo-stimulated conditions (Figure 1B,C), suggesting that stimulated and unstimulated MR assembles with CK1α and CK1ε in a protein–protein complex. CK1δ was only detectable in the nuclear cellular fraction and showed no association with the MR under basal or aldo-treated conditions (Figure S1).

3.2 | CK1 influences GRE activity of corticosteroid receptors

Subsequently, we investigated the influence of CK1 on genomic MR activity in a GRE reporter gene assay. Pharmacological CK1 inhibition with the general CK1 inhibitor D4476 (Figure 2A), the CK1δ and CK1ε specific inhibitor PF-670462 (Figure 2B), and the CK1ε specific inhibitor PF-4800567 (Figure 2C) was measured. We detected a concentration-dependent reduction of basal and aldo-induced genomic MR activity after 24 h of incubation with
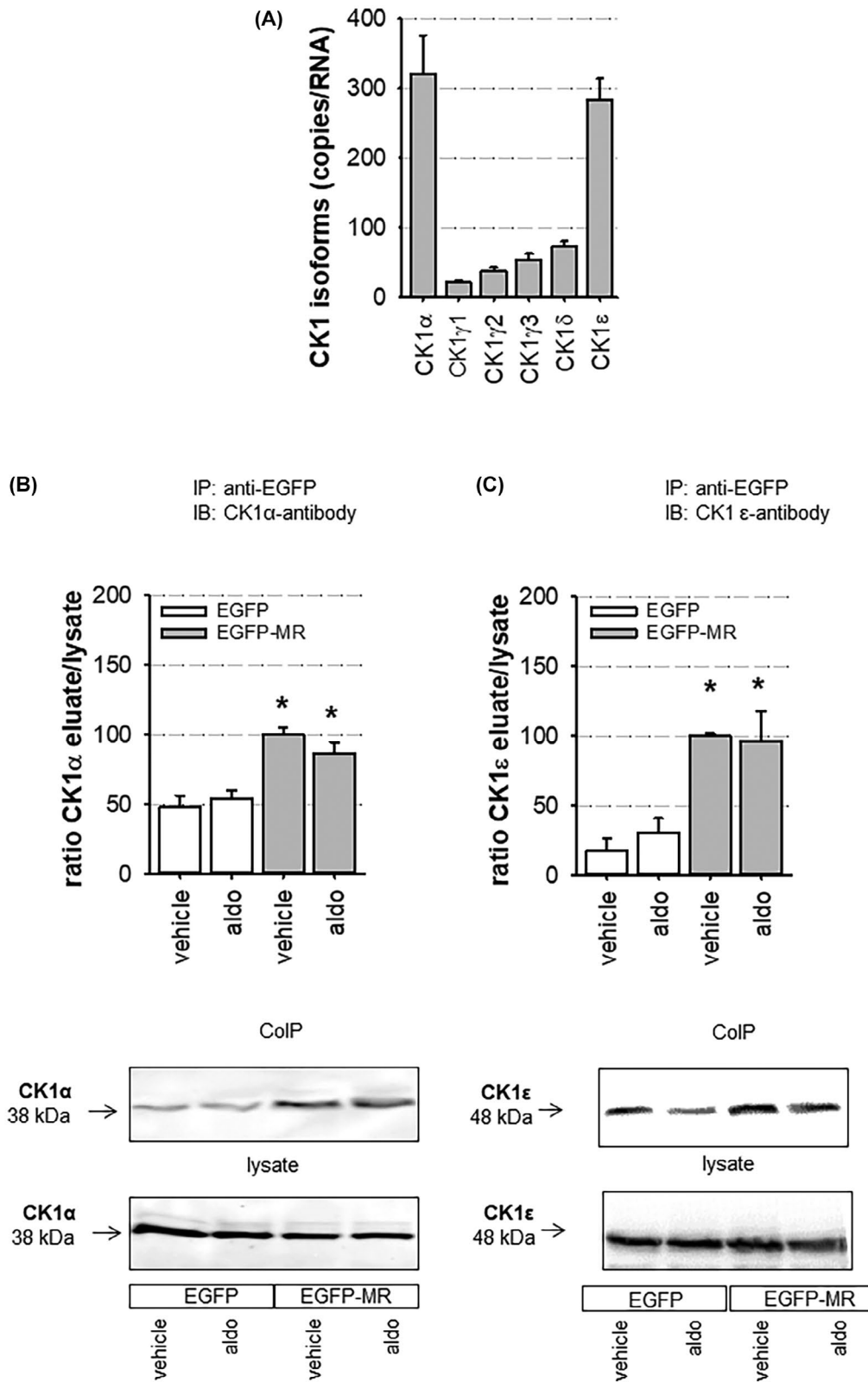
FIGURE 1 MR-CK1 interaction in HEK cells. (A) Expression of different CK1 isoforms was quantified by ddPCR ($N = 3$, $n = 7$–8). (B+C) CoIP experiments of EGFP-/EGFP-MR-transfected HEK cells were performed after aldo (10 nM) stimulation for 1 h. Immunoprecipitation was performed with an anti-EGFP antibody and CK1 isoforms were then detected by Western blot in the eluates ($N = 4$–5; $n = 4$–9; *$p \leq .05$ EGFP vs. the respective EGFP-MR)

all of the respective inhibitors. To compare their suppressive effects over time, we compared the inhibition achieved after 24 and 48 h (Figure 2D). There was no significant difference in the inhibition between the two time points. A toxic effect of the CK1 inhibitors could be excluded because the cell protein content remained largely unchanged (Figure S2). Western blot analyses showed that pharmacological CK1 inhibition did not alter MR protein expression or PTM pattern after 24 h compared to respective controls (Figure 2E). As expected, samples with aldo led to an increase in MR degradation and PTM but D4476 had no additional effect. An unspecific effect of CK1 on our reporter assay system seems unlikely because forskolin-induced CRE-SEAP activity was concentration-dependently increased by D4476 co-treatment (Figure 2F), whereas aldo-induced NFκB-SEAP activity was not affected by incubation with D4476 (Figure 2G). Another approach to clarify the influence of CK1 on genomic MR activity was the use of siRNA against CK1α and CK1ε but unfortunately, CK1α/CK1ε downregulation by siRNA was not sufficient to verify the pharmacological results (Figure S3). The closest relative of the MR, the GR, also induces GRE activity and possesses a high sequence homology to the MR in the DNA- and ligand-binding domain. D4476 caused a comparable inhibition of the corticosteroid-induced genomic GRE activity in EGFP-MR or EGFP-GR transfected HEK cells or in HEK cell with endogenous GR. When endogenous GR activity was inhibited by mifepristone in untransfected HEK cells that also possess no functionally active MR, D4476 exerted no effect on corticosteroid-induced GRE-SEAP activity, demonstrating that the CK1 effect dependents on corticosteroid receptors (Figure 2H). Corticosteroid-induced GR transcriptional activity was reduced by D4476 after 24 and 48 h to nearly the same extent as the respective MR activity (Figure S4A). SEAP-GRE activity after incubation with aldo or aldo and D4476 was comparable after transfection with EGFP-MR and MR without EGFP-tag in HEK cells (Figure S4B). Transactivation activity of a truncated version of the MR lacking the modulatory N-terminal A/B domain and containing only the CDEF domains, which comprise the DNA-binding domain, the hinge region, and the ligand-binding domain, could be inhibited by D4476, PF670464, or PF4800567 to a similar extent as full-length MR after 24 and 48 h of incubation (Figures 2I and S5), indicating that the CDEF domains are sufficient for CK1-induced regulation of genomic MR activity.

3.3 | Several mechanisms lead to CK1-induced altered genomic MR activity

To analyze the mechanism of reduced genomic MR activity in more detail, we investigated nuclear translocation, the cellular distribution of the MR and MR-DNA binding. Time-lapse experiments showed that pharmacological CK1 inhibition by D4476 (10 μM) resulted in a significantly slower aldo-induced nuclear translocation of EGFP-MR ($T_{1/2} = 9.0 \pm 0.7$ min) compared to aldo treatment alone ($T_{1/2} = 6.6 \pm 0.2$ min) (Figure 3A). Additionally, the maximum translocation velocity index increased from 3.4 ± 0.2 min^{-1} to 5.1 ± 0.7 min^{-1} by D4476 treatment (Figure 3B). Cell fractionation studies showed that in the presence of vehicle or D4476, MR resided almost exclusively in the cytosol. Aldo led to a nuclear enrichment of the MR, an effect attenuated by D4476. The fraction of nuclear (15%) and chromatin-associated MR (9%) decreased accordingly (Figure 3C). Finally, we analyzed the MR-DNA interaction after D4476 exposure by EMSA and observed a significant ligand-independent reduction in binding of MR to GRE probes (Figure 3D), indicating that CK1 facilitates MR-DNA binding.

3.4 | CK1-MR interaction influences gene expression

To investigate the functional impact of the CK1-MR interaction, we determined the mRNA expression of the well-known aldo-induced gene *Per-1* and a newly identified aldo-induced gene pleckstrin homology-like domain, family A, member 1 (*Phlda1*) in a tetracyclin-inducible hMR HEK cell clone. MR overexpressing cells incubated with aldo showed a 12.4 fold induction of *Per-1* mRNA expression, which was reduced by D4476 (Figure 3E). The aldo-induced sixfold upregulated *Phlda1* expression was also reduced significantly by D4476 (Figure 3F). Overexpression of MR in the stable HEK clone was approximately eightfold (Figure S6). As further indication that the inhibition of MR signaling by CK1 inhibitors is also relevant in other cell types, D4476 also inhibited MR transcriptional activity in EA.hy926 cells that possess endothelial characteristics (Figure S7A). Aldo-induced genes TSC22D3 (GILZ) and PDK4 could be inhibited by 10 μM D4476 in EA.hy926 cells expressing endogenous MR (Figure S7B,C).

3.5 | CK1 can directly phosphorylate serine and threonine residues of the MR in vitro

We performed peptide microarrays experiments to identify directly CK1 phosphorylated MR residues as described previously.[7] Ten CK1-induced phosphorylation sites containing a CK1 consensus site were detected by peptide microarray according to our selection criteria (see Material and Methods), two of which were located in the functionally relevant CDEF domain for the MR-CK1
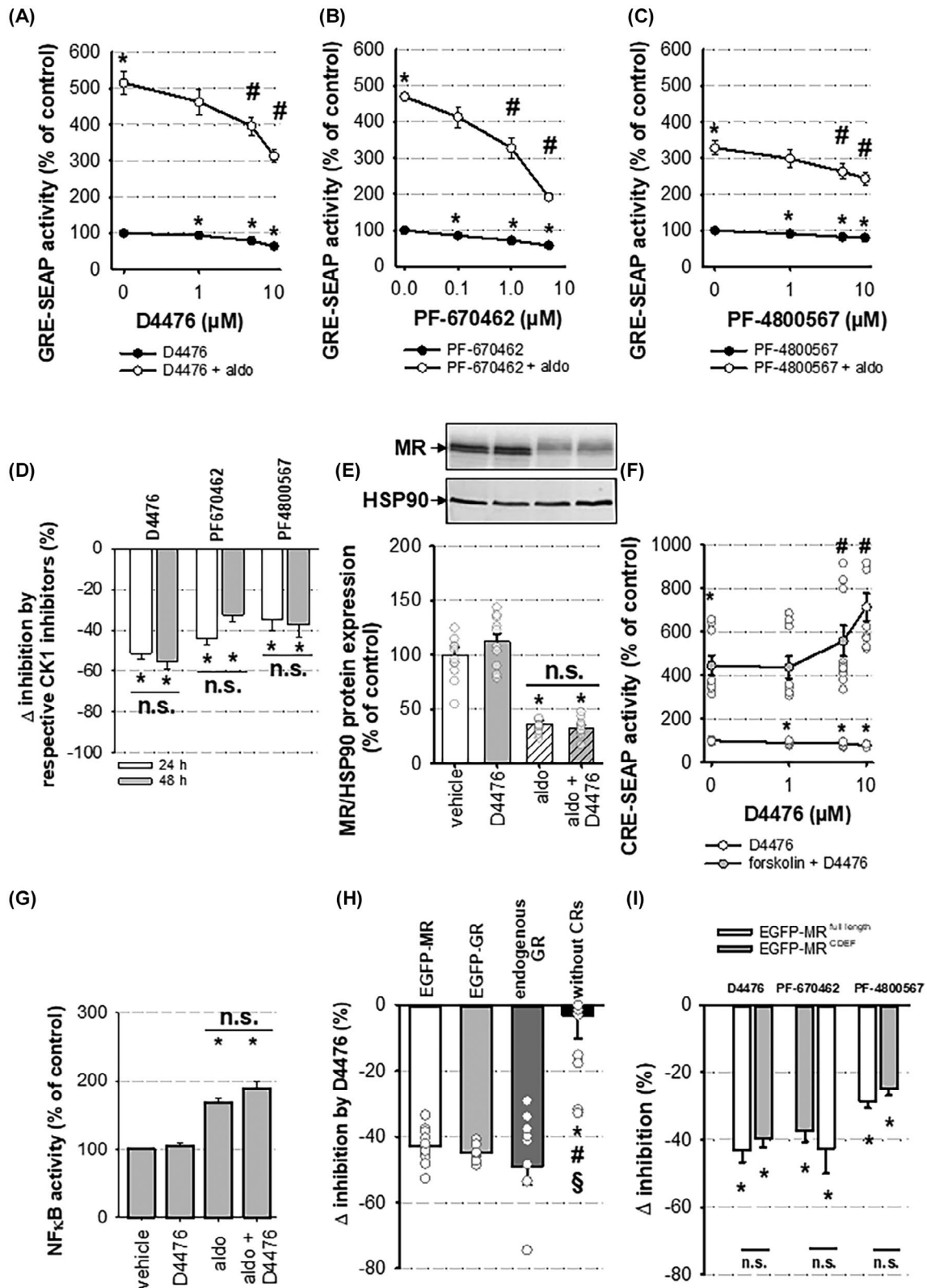
interaction (Figure 4A). MR-T800 and MR-S936 with the canonical consensus sequences D/E-X-X-S*/T* were then investigated further with respect to their influence on the genomic MR activity by mutating the serine and threonine residue T800 and S936 into non-phosphorylatable alanine (phospho-deficient mutants).

3.6 | CK1-phosphorylated amino acids T800 and S936 influence genomic MR activity and nuclear translocation

Both MR mutants showed an approximately fourfold reduced expression compared to MR-WT (Figure 4B).

FIGURE 2 Influence of pharmacological CK1 inhibition on hormone response element activity and protein expression of corticosteroid receptors. (A–C) Pharmacological CK1 inhibitors (D4476, PF-670462, PF-4800567) diminished aldo (10 nM)-induced genomic MR activity in MR-transfected HEK cells after 24 h as determined by GRE-SEAP reporter gene assay ($N = 3–7$; $n = 6–21$; *$p \leq .05$ vs. MR vehicle; #$p \leq .05$ MR aldo vs. MR aldo + respective inhibitor). (D) Comparison of the inhibitory effects of pharmacological CK1 inhibitors (10 μm D4476, 1 μM PF670462, 10 μM PF4800567) on genomic MR activity after 24 h and 48 h treatment ($N = 3–7$; $n = 6–21$; *$p \leq .05$ MR aldo (10 nM) vs. MR aldo + respective inhibitor). (E) Aldo stimulation (10 nM) of MR-transfected HEK cells led to PTM and degradation of the receptor, which was unaffected by D4476 (10 μM) co-treatment after 24 h as analyzed by Western blot ($N = 3$; $n = 5–6$; *$p \leq .05$ vs. MR vehicle/D4476). (F) D4476 increased forskolin (3 μM)-induced CRE-SEAP activity concentration-dependently in untransfected HEK cells after 24 h ($N = 3$; $n = 6–9$; *$p \leq .05$ vs. vehicle; #$p \leq .05$ forskolin vs. forskolin + respective D4476 concentration). (G) Aldo (10 nM)-induced MR activation increased NF-κB reporter gene activity, which was unaffected by D4476 (10 μM) co-treatment after 24 h ($N = 3$; $n = 9$; *$p \leq .05$ MR vehicle/D4476 vs. MR aldo/MR aldo + D4476). (H) GRE-SEAP activity of aldo (10 nM)-stimulated MR, dexa (10 nM)-stimulated EGFP-GR and endogenous GR were determined by D4476 (10 μM) co-treatment for 24 h. Δ inhibition of GRE-SEAP activity by D4476 co-treatment was calculated and compared with the inhibitory effect of D4476 when the endogenous GR was blocked by mifepristone (1 μM) ($N = 3–6$; $n = 6–18$; *$p \leq .05$ MR vs. without CR; #$p \leq .05$ GR vs. without CR; §$p \leq .05$ endogenous GR vs. without CR). (I) inhibition of aldo (10 nM)-induced genomic MR activity by D4476 (10 μM), PF-670462 (5 μM) or PF-4800567 (10 μM) was analyzed for EGFP-MR-WT and truncated EGFP-MR-CDEF by GRE-SEAP reporter gene assay after 48 h ($N = 3$; $n = 6–9$; *$p \leq .05$ MR$^{full length}$ aldo/MR^{CDEF}aldo vs. MR$^{full length}$ aldo + respective inhibitor/MR^{CDEF}aldo + respective inhibitor)

When increasing the transfected plasmid concentration fourfold compared to MR-WT, the protein expression of the T800A mutant was slightly higher whereas the protein expression of the S936A mutant was comparable to MR-WT (Figure 4C). These conditions were then used to test the transcriptional activity of the MR mutants by GRE-SEAP reporter assays. Aldo (1 nM)-induced genomic MR activity was reduced by 46% for MR-T800A, whereas the genomic activity of MR-S936A was unchanged compared to MR-WT (Figure 4D,E). Analysis of the EC$_{50}$ values showed that the apparent affinity of MR T800A is reduced compared to WT-MR (Figure 4F). Furthermore, T800 is conserved among orthologues from reptiles to mammals in contrast to S936 (Figure 5A,B). Time-lapse experiments showed that ligand-induced cytosolic nuclear shuttling of MR-T800A (8.5 min ± 1.0) and MR-S936A (8.6 min ± 0.8) was slower compared to MR-WT (6.4 min ± 0.3/6.6 min ± 0.2—Figure 5C,D). As before, D4476 increased the half life time of MR-WT but it exerted no additional effect on nuclear shuttling of MR-T800A (8.7 min ± 1) or MR-S936A (8.7 min ± 1) (Figure 5C,D). The maximum translocation velocity indices were not altered neither for MR-T800A (4.1 min ± 0.5) nor for MR-S936A (3.9 min ± 0.5) compared to MR-WT (3.5 min ± 0.3) (Figure 5E,F). Cell fractionation experiments showed that the amount of mutated MR-T800A in the individual cell fractions did not differ from MR-WT (Figure 5G) indicating that the single amino acid T800 is not sufficient to lead to a decreased steady-state MR accumulation in the nucleus as is the case with the pharmacological inhibition of CK1 (Figure 3C).

3.7 | MR-associated proteins are predicted to be influenced by CK1

MR pull-down experiments followed by TMT labeling and quantitative mass spectrometric analyses were performed in search for MR-associated co-factors. 104 MR-associated proteins were identified on the basis of the quantification criteria described in the Materials and Methods section and are summarized in Table S2. Among the MR-associated proteins, several known MR interaction partners like HSP90 and p23 as well as NOLC1 (nucleolar and coiled-body phosphoprotein 1) and TCOF1 (treacle protein) were detected (Figure 6A). We further investigated whether these MR-associated proteins can be phosphorylated by CK1 by *in silico* prediction using Netphos3.1. As depicted in Figure 6B, 79 MR-associating proteins possess a least one putative CK1 phosphorylation site, 30 at least five, and 7 more than 10 possible CK1 phosphorylation sites. For TCOF1 and NOLC1, 45 respective 21 putative CK1 phosphorylation sites were predicted. The potential influence of these two MR-associated proteins on genomic MR activity will be analyzed in future studies.

4 | DISCUSSION

Previously, no evidence existed for CK1-induced modulation of MR function. Pharmacological CK1 inhibitors are currently used as therapeutics for neurodegenerative diseases and tumors and extending these applications to other disorders, like, for example, cardiovascular diseases, is an attractive possibility.[12,13,21] We now demonstrate that MR interacts with CK1α and CK1ε in a protein-protein complex and that pharmacological CK1 inhibition modulates genomic MR activity, indicating that CK1 facilitates MR actions. To identify the CK1 isoform responsible for the described effects we utilized different isoform-specific CK1 inhibitors since a sufficient knock-down of the highly abundant CK1 isoforms by siRNA could not be achieved. D4476, a CK1 inhibitor which inhibits all isoforms approximately equally,[22] led to a 50% reduction of MR activity. PF670462, as well as PF-4800567, belong to the late
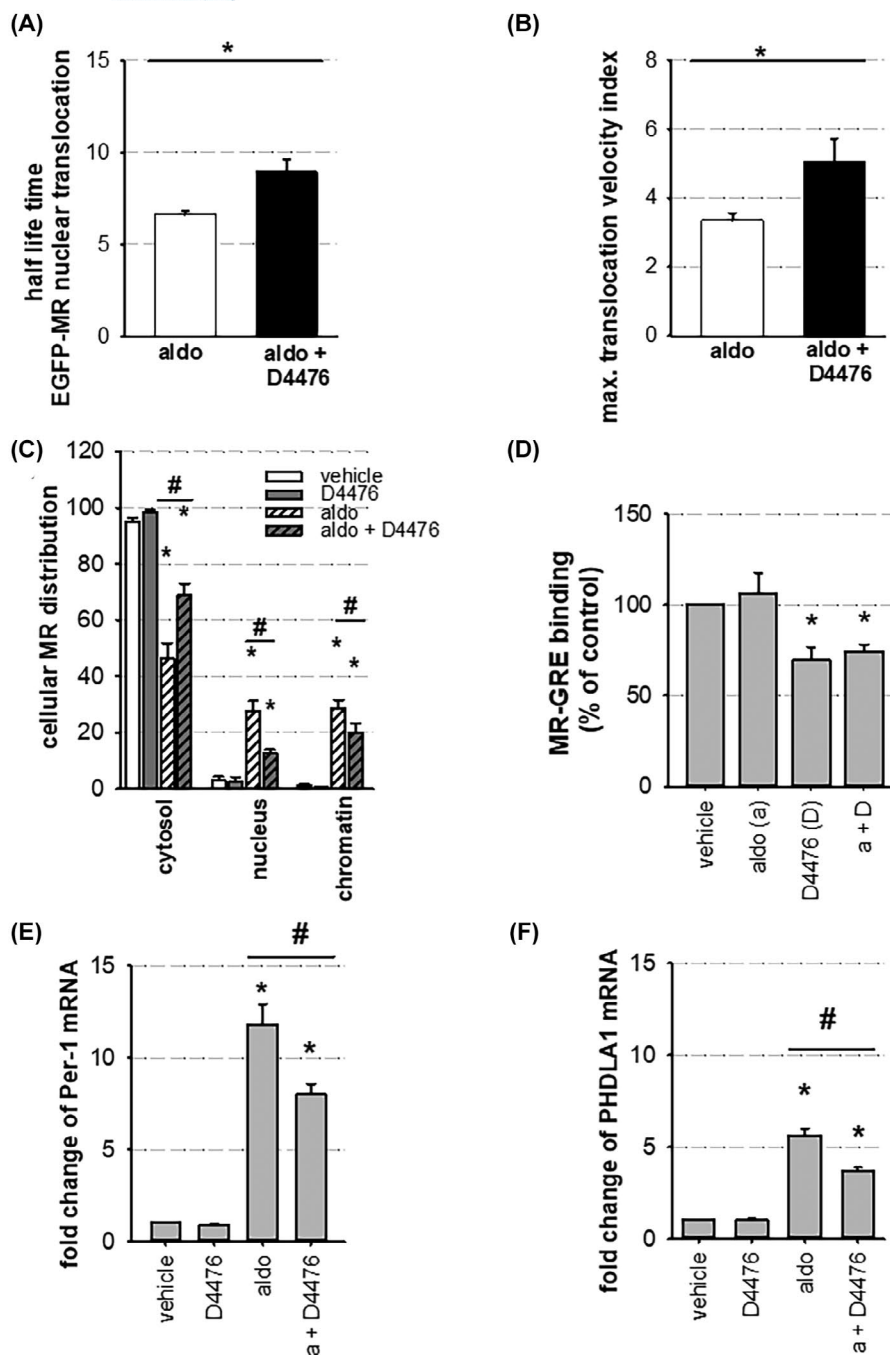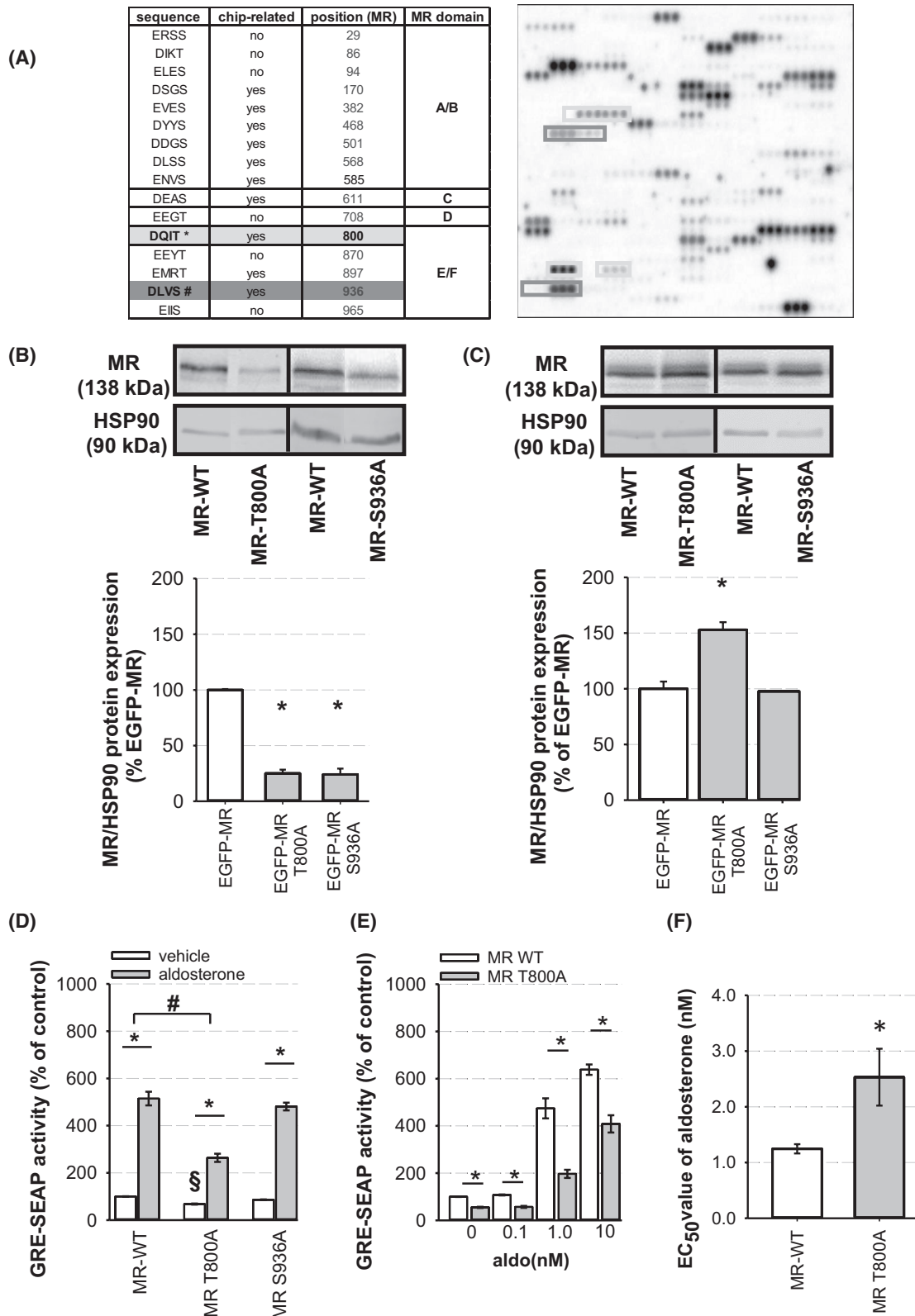
(A)

(B)

(C)

(D)

(E)

(F)

FIGURE 3 Mechanism of diminished genomic MR activity by pharmacological CK1 inhibition and consequences for gene expression. (A) Half life time and (B) maximum translocation velocity index of aldo (10 nM)-induced nuclear MR translocation were determined by time-lapse experiments utilizing MR-transfected HEK with or without 1 h preincubation with 10 μM D4476 ($N = 16$–18; $n = 16$–18; *$p ≤ .05$ as indicated). (C) EGFP-MR transfected HEK cells were treated with vehicle, aldo (10 nM) $±$ D4476 (10 μM) for 1 h followed by cell fractionation and Western blot analysis. ($N = 3$; $n = 8$–9; *$p ≤ .05$ vs. vehicle; #$p ≤ .05$ as indicated). (D) MR-GRE binding was analyzed by EMSA using EGFP-MR transfected HEK cell lysates, which were treated with $±$ aldo (10 nM) $±$ D4476 (10 μM) for 1 h. ($N = 3$–4; $n = 3$–4; *$p ≤ .05$ MR vehicle vs. MR D4476; *$p ≤ .05$ MR aldo vs. MR aldo + D4476). (E+F) Quantification of *Per-1* and *Phlda1* mRNA expression after treatment of tetracyclin-inducible MR HEK cells with vehicle, aldo (10 nM), D4476 (10 μM) or aldo + D4476 for 6 h ($N = 3$; $n = 8$–9; *$p ≤ .05$ vs. vehicle; #$p ≤ .05$ as indicated)

FIGURE 4 Identification and characterization of direct CK1-induced phosphorylation residues of the MR. (A) *In silico* predicted CK1 phosphorylation sites of the MR and their CK1 consensus sequences are shown in the table (left panel), together with their localization in the MR domains. Ten CK1-induced phosphorylation sites of the MR were detected (chip-related: yes) by peptide microarray (right panel). Four of these CK1 phosphorylation sites were located in the relevant CDEF domain of the MR and only two T800 (*) and S936 (#) met the defined criteria and were analyzed further. (B) MR protein expression of MR-WT-transfected HEK cells in comparison to MR-T800A- and MR-S936A- transfected HEK cells was analyzed by Western blot ($N = 4$; $n = 5$–7; *$p ≤ .05$ respective MR mutant vs. MR-WT). (C) HEK cells were transiently transfected with 4-fold increased amounts of plasmid for MR-T800A and MR-S936A (1 μg/cm²) compared to MR WT (0.25 μg/cm²), and protein expression was quantified by Western blot ($N = 3$; $n = 6$–9; *$p ≤ .05$ MR-T800A vs. MR-WT). (D) Aldo (1 nM)-induced genomic activity of MR-T800A and MR-S936A was analyzed in comparison to MR-WT by GRE-SEAP reporter gene assay after 24 h. ($N = 3$; $n = 6$–9; §$p ≤ .05$ MR-T800A vehicle vs. MR-WT vehicle; *$p ≤ .05$ aldo vs. vehicle as indicated, #$p ≤ .05$ aldo-induction of MR-T800A vs. MR-WT). (E) Genomic MR activities of MR-WT and MR-T800A were determined by GRE-SEAP reporter gene assay after concentration-dependent aldo stimulation for 24 h. ($N = 3$; $n = 6$–9; *$p ≤ .05$ as indicated). (F) EC$_{50}$ values were determined from (E) for MR-WT and MR-T800A ($N = 3$–6; $n = 3$–6; *$p ≤ .05$)

state CK1 inhibitors.[12] PF-670462 is described as a specific CK1δ/ε inhibitor and reduced transcriptional MR activity by 44%. Finally, we tested a CK1ε specific inhibitor PF4800567, which also reduced genomic MR activity up to 38%. Considering that the MR is associated with CK1α

and CK1ε in a protein–protein complex, it suggests that CK1ε is the most relevant MR co-activator in our HEK cell model. Non-specific toxic or inhibitory transcriptional effects of D4476 were excluded by showing that basal GRE-SEAP activity in the absence of corticosteroid receptors
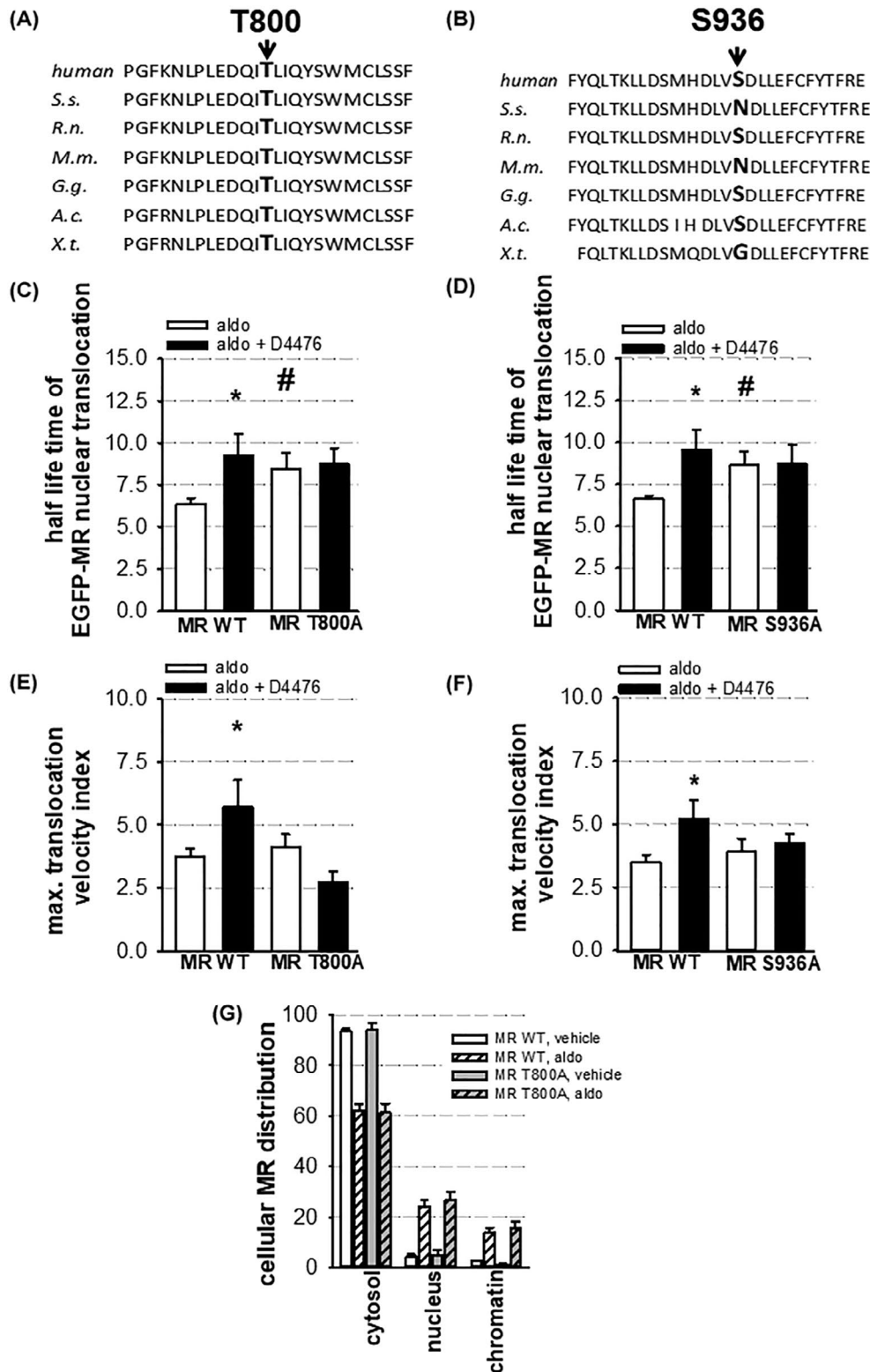
(A)

sequence	chip-related	position (MR)	MR domain
ERSS	no	29	
DIKT	no	86	
ELES	no	94	
DSGS	yes	170	
EVES	yes	382	A/B
DYYS	yes	468	
DDGS	yes	501	
DLSS	yes	568	
ENVS	yes	585	
DEAS	yes	611	C
EEGT	no	708	D
DQIT *	yes	800	
EEYT	no	870	
EMRT	yes	897	E/F
DLVS #	yes	936	
EIIS	no	965	

(B)

MR (138 kDa)
HSP90 (90 kDa)

MR-WT MR-T800A MR-WT MR-S936A

MR/HSP90 protein expression (% EGFP-MR)

EGFP-MR EGFP-MR T800A EGFP-MR S936A

(C)

MR (138 kDa)
HSP90 (90 kDa)

MR-WT MR-T800A MR-WT MR-S936A

MR/HSP90 protein expression (% of EGFP-MR)

EGFP-MR EGFP-MR T800A EGFP-MR S936A

(D)

GRE-SEAP activity (% of control)

□ vehicle ■ aldosterone

MR-WT MR T800A MR S936A

(E)

GRE-SEAP activity (% of control)

□ MR WT ■ MR T800A

aldo(nM): 0, 0.1, 1.0, 10

(F)

EC_{50} value of aldosterone (nM)

MR-WT MR T800A

(A) T800

human PGFKNLPLEDQI**T**LIQYSWMCLSSF
S.s.   PGFKNLPLEDQI**T**LIQYSWMCLSSF
R.n.   PGFKNLPLEDQI**T**LIQYSWMCLSSF
M.m.   PGFKNLPLEDQI**T**LIQYSWMCLSSF
G.g.   PGFKNLPLEDQI**T**LIQYSWMCLSSF
A.c.   PGFRNLPLEDQI**T**LIQYSWMCLSSF
X.t.   PGFRNLPLEDQI**T**LIQYSWMCLSSF

(B) S936

human FYQLTKLLDSMHDLV**S**DLLEFCFYTFRE
S.s.   FYQLTKLLDSMHDLV**N**DLLEFCFYTFRE
R.n.   FYQLTKLLDSMHDLV**S**DLLEFCFYTFRE
M.m.   FYQLTKLLDSMHDLV**N**DLLEFCFYTFRE
G.g.   FYQLTKLLDSMHDLV**S**DLLEFCFYTFRE
A.c.   FYQLTKLLDS I H DLV**S**DLLEFCFYTFRE
X.t.   FQLTKLLDSMQDLV**G**DLLEFCFYTFRE

FIGURE 5 Characteristics of CK1-phospho-deficient MR mutants. (A+B) Conservation of T800 and S936 among MR orthologous. *S.s.*, *Saimiri sciureus (common squirrel monkey)*; *R.n.*, *Rattus norvegicus (brown rat)*; *M.m.*, *Mus musculus (house mouse)*; *G.g.*, *Gallus gallus (red junglefowl)*; *A.c.*, *Anolis carolinensis (green anole)*; *X.t.*, *Xenopus tropicalis (western clawed frog)*. (C–F) Half life time (C+D) and maximum translocation velocity index (E+F) of aldo (10 nM)-induced nuclear MR translocation were determined by time-lapse experiments utilizing EGFP-MR-WT-, EGFP-MR-T800A- and EGFP-MR-S936A-transfected HEK cells ± 1 h pretreatment with D4476 (10 μM). ($N = 5$–12; $n = 5$–12; *$p \leq .05$ MR WT aldo vs. MR aldo + D4476; #$p \leq .05$ MR-WT aldo vs. MR T800A aldo/MR S936A). (G) Cell fractionation was performed using EGFP-MR and EGFP-MR-T800A transfected HEK cells, which were treated $\pm$ aldo (10 nM) for 1 h followed by Western blot analysis ($N = 3$; $n = 8$–9)
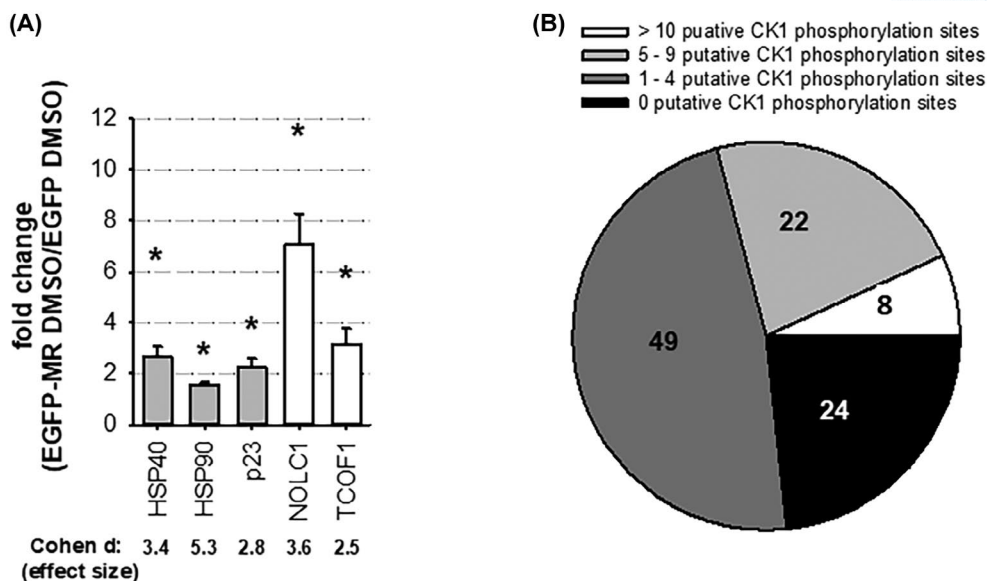
(A)

(B)

FIGURE 6 Analysis of MR-associated co-factors. (A) LC/MS/MS analysis identified 104 MR-interacting proteins including HSP40,-90, p23, but also novel MR-binding partners, such as NOLC1 and TCOF1, which contain a high number of putative CK1 phosphorylation sites ($N = 4$; $n = 4$; *$p \leq .05$ EGFP-MR vs. EGFP). (B) Classification of MR interacting proteins with respect to their ability to be directly phosphorylated by CK1 utilizing Netphos 3.1

was not affected and that forskolin-induced CRE-SEAP activity was even enhanced by D4476. Horiuchi et al. and Shanware et al. already described that CK1 isoforms act as co-repressors of CREB function. CK1 and CK2 phosphorylation sites are conserved in *Drosophila* CREB and have been shown to inhibit its DNA binding activity.[23] CK1-mediated phosphorylation of CREB is a prerequisite for ATM-protein kinase–dependent phosphorylation on Ser-121 during genotoxic stress, switching CREB into a low CBP-binding state with reduced transcriptional CREB activity.[24] No influence of CK1 on NF-κB-activity of the MR was found, suggesting that only transcriptional activity at GRE sites is affected. Inhibitor studies showed that the NTD of the MR is not required for D4476/PF670462/PF4800567-induced repression of MR transactivation activity, indicating that the MR-CK1 interaction takes place in the CDEF domains of the receptor. The MR's ligand and DNA binding domain in this region is highly homologous to that of the GR, and only the short hinge region in between is poorly conserved. Accordingly, CK1 inhibition by D4476 also reduced genomic GR activity. An influence of CK1 on the genomic activity of other nuclear receptors has been shown for ERα, which is phosphorylated and stimulated by CK1δ.[18] Known MR co-regulators bind either to the NTD via an "unidentified" motif[25] or to the AF-2 region in the LBD of the MR (which is part of the CDEF construct) via one or more L-XX-LL motifs.[26,27] None of the CK1 isoforms contains a L-XX-LL motif with which it could bind to MR. However, it is known that CK1 can also associate with proteins that lack such

a motif (e.g., axin), which indicates that other unknown CK1-binding motifs exist.[14] An interaction of MR and CK1 in a cytosolic multi-protein complex seems likely, as described for β-catenin and the circadian regulatory protein cryptochrome.[14,28] Thereby, a change in MR functionality could occur caused by direct CK1-induced phosphorylation of MR residues as shown by peptide microarrays and/or indirectly via the CK1-induced phosphorylation of MR co-regulatory proteins. For ERα it was shown that CK1δ can interact and phosphorylate ERα as well as the ERα co-regulator SRC-3 in a protein-protein complex, resulting in an increased ERα transcriptional activity accompanied by elevated ERα protein degradation.[18]

The importance of single MR residues as CK1 phosphorylation sites was investigated with phospho-deficient MR mutants. Treatment of MR-WT with D4476 as well as the mutants MR-T800A and S936A showed a delayed nuclear translocation of the MR. These data suggest that the direct CK1-induced phosphorylation of MR at T800 and S936 promotes the nuclear translocation of the MR. When testing the MR phospho-deficient mutants, D4476 no longer had an additional effect on trafficking of the MR. Nuclear MR import is a mechanism that depends on the nuclear localization signal (NLS). MR possesses a NLS1, which is a core of basic acids that extends beyond the C-terminal end of the DBD, a second NLS2 within the LBD, which is dependent on the LBD conformation,[4] and a third NLS0 located in the NTD.[29] Piwien Pilipuk et al. showed that the exposure of typical NLSs is not sufficient to guarantee efficient nuclear MR translocation and

that alternative import mechanism exists that is clearly HSP90- and NLS1-independent.[29] The CK1-induced phosphorylation of T800 and S936 could be part of such a mechanism occurring in the NLS2, which is crucial for the import of MR into the nucleus. Yang and Sale showed that CK1-induced phosphorylation of dynein is involved in retrograde cellular transport, providing a possible molecular explanation.[30] Inhibition of CK1 with D4476, on the contrary, resulted in a reduced accumulation of MR in the nucleus upon aldo stimulation, but this effect could not be reproduced with the MR-T800A mutant. The overall relevance of the change in the nuclear-cytoplasmic shuttling of the mutant, therefore, remains unclear.

Our results indicate that CK1 needs to either phosphorylate several MR phosphorylation sites simultaneously and/or additional MR co-regulators to support nuclear accumulation. In addition, our inhibitory CK1 experiments suggest that CK1-induced phosphorylation of the MR or MR co-regulators leads to an increased binding of the MR to DNA as shown by EMSA experiments. Using the mutants, we show that the highly conserved CK1 phosphorylation site T800 modulates genomic MR activity positively, whereas the little conserved S936A site is not involved in the regulation of transcriptional activity. T800 is conserved from mammals to fish and is also conserved for GR and progesterone receptors. Based on the published crystal structures, both amino acids appear to be outwardly facing and therefore accessible to a protein complex for phosphorylation. Although ligand binding was not directly studied for MR-T800A, the dose-response to ligand in the transactivation assay concurs with a decrease in ligand affinity. The additional change in MR stability could be the result of an altered interaction with the HSP90 chaperone complex, which keeps the MR in a conformation capable of ligand binding and prevents degradation or it could be the result of structural changes induced by the exchange in amino acid. The inhibitory effect of pharmacological CK1 inhibition on aldo-induced MR activity can only be partly explained by the CK1 induced phosphorylation of T800 but again other mechanisms such as CK1-induced phosphorylation of MR co-regulators and multiple CK1-induced MR phosphorylation may be also involved as described for ERα.[18]

Two interesting potential MR co-regulatory proteins determined by LC/MS/MS are NOLC1 and TCOF1, which are paralogs.[31] Both proteins have a high content of acidic amino acids and are predicted to be phosphorylated by CK1. NOLC1, a phosphoprotein, was first identified as a nuclear localization signal protein, which rapidly shuttles as a chaperone into the nucleus[32,33] and can therefore probably facilitate MR translocation into the nucleus. For TCOF1 a similar shuttling between cytosol and nucleus was described.[34] Furthermore, PKA-phosphorylated

NOLC1 also associates with the general transcription factor TFIIB and furthers gene transcription.[35] The exact influence of CK1 on the function of MR co-regulators needs to be explored. CK1-induced phosphorylation of MR residues and/or MR co-regulators culminates in an enhanced transcriptional MR activity demonstrated by the robust aldo-induced mRNA expression of *Per-1* and *Phlda1* after 6 h. *Per-1* is a circadian clock gene and represents a typical early aldo-induced MR target gene, which has an impact
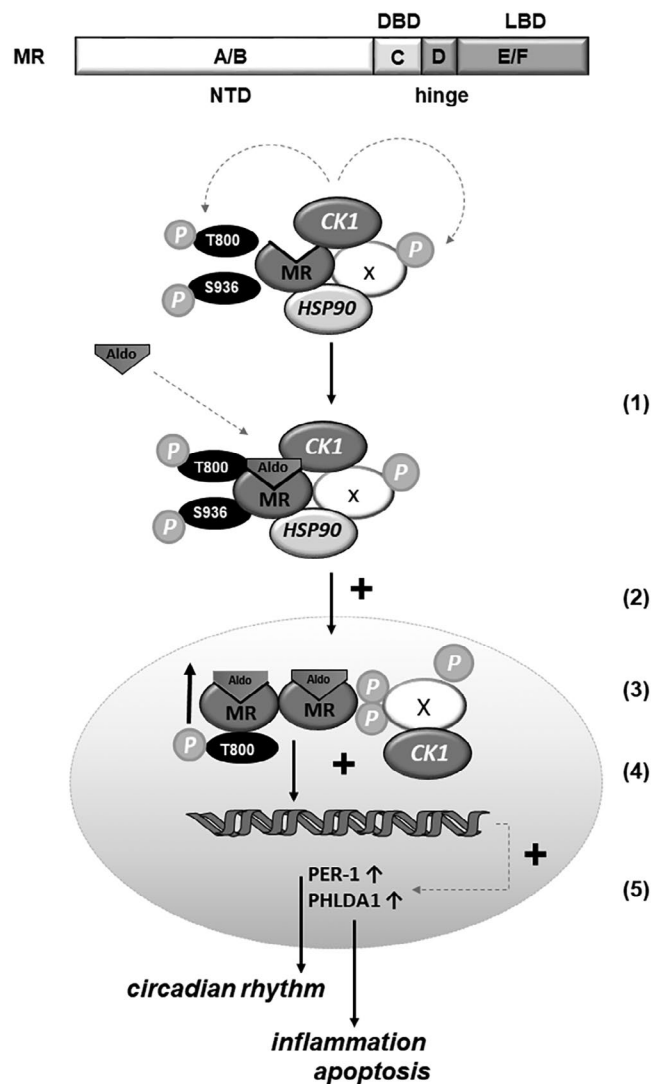

FIGURE 7 Working model: Influence of CK1 as a positive regulator of genomic MR activity: (1) Under basal and ligand-stimulated conditions, CK1 and MR are associated in a protein-protein complex. CK1 directly phosphorylates the MR at residue T800 and S936 and also phosphorylates MR co-regulatory proteins. (2) CK1-induced phosphorylation of MR-T800 and -S936 facilitates nuclear translocation of the MR. (3) CK1-induced phosphorylation of MR co-regulatory proteins elevates the amount of nuclear MR in the nucleus, augments MR-DNA interactions, and increases the expression of MR target genes like *PER-1* and *PHLDA1*. NTD, N-terminal domain; LBD, ligand binding domain; DBD, DNA binding domain

on the regulation of many physiological functions such as blood pressure and renal functions through regulating αENaC expression.[15,16,36] Aldo-induced *Per-1* mRNA expression was also observed in different kidney cells e.g., the inner medullary collecting duct cells (IMCD-3), renal epithelial cells (mIMCD-K2), cortical collecting duct cells (mpkCCD), and HK-GFP MR cells.[15,36] We hypothesize that the nuclear import of the MR mediated by CK1 supports *Per1* mRNA expression since inhibition of enzymatic CK1 activity by D4476 leads to a 33% reduction in *Per1* mRNA expression. We also identified a new aldo-induced MR target gene, *Phlda1*, whose mRNA expression is also CK1-dependent. Increased expression of PHLDA1 has been described in cardiomyocytes under oxidative stress conditions, resulting in increased radical production and apoptosis rate of cardiomyocytes.[37] In addition, Han et al. showed that the expression of PHLDA1 is enhanced by inflammatory stimuli in microglia cells and aggravates the inflammatory situation.[38]

Overall, in the present study, we identified a novel role of CK1 as a direct (e.g., T800; S936) and/or indirect regulator of MR (and GR) transcriptional activity as indicated in our working model (Figure 7). CK1-induced phosphorylation of the MR (i) fosters nuclear MR translocation, (ii) increases nuclear MR levels, and (iii) augments MR-DNA interaction. Functionally, this leads to an increased expression of aldo-induced MR target genes via CK1-dependent mechanisms, which can lead to alterations in the circadian rhythm (*Per-1*) and cellular stress level (*Phlda1*). Future investigations are necessary to investigate the effect of the different CK1 isoforms on MR signaling in more physiologic settings and to clarify the circumstances under which this interaction plays a role. Overall, CK1 activity and or expression has been shown to be regulated by posttranslational modifications, posttranscriptional regulation (alternative splicing and microRNAs), subcellular compartmentalization, and allosteric mechanisms. Stress but also signaling pathways have been implicated in the regulation of CK1.[39–42] Consequently, we hypothesize that changes in micromilieu or signaling intermediates may lead to changes in CK1 activity, which then affects the intensity with which the MR responds to ligand in different tissues. A similar regulation also seems feasible for the GR., which is derived from a common ancestral receptor and shares some ligands and hormone-response elements with the MR.

ACKNOWLEDGMENTS

DISCLOSURES

AUTHOR CONTRIBUTIONS

Stefanie Ruhs designed experiments, analyzed data, and wrote the paper. Bruno Griesler and Ralf Huebschmann performed and analyzed experiments. Nicole Straetz performed experiments. Katharina Stroedecke provided new research reagents and analytic tools. Antonia Masch and Mike Schutkowski conducted and evaluated the peptide microarray experiments. Christian Ihling and Andrea Sinz performed and evaluated the TMT labeling and LC/MS/MS experiments. Michael Gekle and Claudia Grossmann designed research, analyzed data, and edited the manuscript.

ORCID

Claudia Grossmann https://orcid.org/0000-0003-2026-1980

REFERENCES

1. Gadaleta RM, Magnani L. Nuclear receptors and chromatin: an inducible couple. *J Mol Endocrinol*. 2014;52:R137-R149.
2. Lother A, Moser M, Bode C, Feldman RD, Hein L. Mineralocorticoids in the heart and vasculature: new insights for old hormones. *Annu Rev Pharmacol Toxicol*. 2015;55:289-312.
3. Wang CH, Hung PW, Chiang CW, et al. Identification of two independent SUMO-interacting motifs in Fas-associated factor 1 (FAF1): implications for mineralocorticoid receptor (MR)-mediated transcriptional regulation. *Biochim Biophys Acta Mol Cell Res*. 1866;2019:1282-1297.
4. Walther RF, Atlas E, Carrigan A, et al. A serine/threonine-rich motif is one of three nuclear localization signals that determine unidirectional transport of the mineralocorticoid receptor to the nucleus. *J Biol Chem*. 2005;280:17549-17561.
5. Yang J, Young MJ. The mineralocorticoid receptor and its coregulators. *J Mol Endocrinol*. 2009;43:53-64.
6. Faresse N. Post-translational modifications of the mineralocorticoid receptor: how to dress the receptor according to the circumstances? *J Steroid Biochem Mol Biol*. 2014;143:334-342.
7. Ruhs S, Straetz N, Quarch K, et al. Modulation of transcriptional mineralocorticoid receptor activity by casein kinase 2. *Sci Rep*. 2017;7:15340.
8. Weigel NL. Steroid hormone receptors and their regulation by phosphorylation. *Biochem J*. 1996;319(Pt 3):657-667.
9. Kino T, Jaffe H, Amin ND, et al. Cyclin-dependent kinase 5 modulates the transcriptional activity of the mineralocorticoid receptor and regulates expression of brain-derived neurotrophic factor. *Mol Endocrinol*. 2010;24:941-952.
10. Shibata S, Rinehart J, Zhang J, et al. Mineralocorticoid receptor phosphorylation regulates ligand binding and renal response to volume depletion and hyperkalemia. *Cell Metab*. 2013;18:660-671.
11. Qiao Y, Chen T, Yang H, et al. Small molecule modulators targeting protein kinase CK1 and CK2. *Eur J Med Chem*. 2019;181:111581.
12. Cozza G, Pinna LA. Casein kinases as potential therapeutic targets. *Null*. 2016;20:319-340.

13. Schittek B, Sinnberg T. Biological functions of casein kinase 1 isoforms and putative roles in tumorigenesis. *Mol Cancer.* 2014;13:231.

14. Cheong JK, Virshup DM. Casein kinase 1: complexity in the family. *Int J Biochem Cell Biol.* 2011;43:465-469.

15. Gumz ML, Stow LR, Lynch IJ, et al. The circadian clock protein Period 1 regulates expression of the renal epithelial sodium channel in mice. *J Clin Invest.* 2009;119:2423-2434.

16. Richards J, Greenlee MM, Jeffers LA, et al. Inhibition of alphaENaC expression and ENaC activity following blockade of the circadian clock-regulatory kinases CK1delta/epsilon. *Am J Physiol Renal Physiol.* 2012;303:F918-F927.

17. Okamura H, Garcia-Rodriguez C, Martinson H, Qin J, Virshup DM, Rao A. A conserved docking motif for CK1 binding controls the nuclear localization of NFAT1. *Mol Cell Biol.* 2004;24:4184-4195.

18. Giamas G, Castellano L, Feng Q, et al. CK1delta modulates the transcriptional activity of ERalpha via AIB1 in an estrogen-dependent manner and regulates ERalpha-AIB1 interactions. *Nucleic Acids Res.* 2009;37:3110-3123.

19. Grossmann C, Freudinger R, Mildenberger S, Husse B, Gekle M. EF Domains are sufficient for nongenomic mineralocorticoid receptor actions. *J Biol Chem.* 2008;283:7109-7116.

20. Ihling A, Ihling CH, Sinz A, Gekle M. Acidosis-induced changes in proteome patterns of the prostate cancer-derived tumor cell line AT-1. *J Proteome Res.* 2015;14:3996-4004.

21. Yasojima K, Kuret J, DeMaggio AJ, McGeer E, McGeer PL. Casein kinase 1 delta mRNA is upregulated in Alzheimer disease brain. *Brain Res.* 2000;865:116-120.

22. Rena G, Bain J, Elliott M, Cohen P. D4476, a cell-permeant inhibitor of CK1, suppresses the site-specific phosphorylation and nuclear exclusion of FOXO1a. *EMBO Rep.* 2004;5:60-65.

23. Horiuchi J, Jiang W, Zhou H, Wu P, Yin JCP. Phosphorylation of conserved casein kinase sites regulates cAMP-response element-binding protein DNA binding in drosophila. *J Biol Chem.* 2004;279:12117-12125.

24. Shanware NP, Trinh AT, Williams LM, Tibbetts RS. Coregulated ataxia telangiectasia-mutated and casein kinase sites modulate cAMP-response element-binding protein-coactivator interactions in response to DNA damage. *J Biol Chem.* 2007;282:6283-6291.

25. Pascual-Le Tallec L, Simone F, Viengchareun S, Meduri G, Thirman MJ, Lombès M. The elongation factor ELL (eleven-nineteen lysine-rich leukemia) is a selective coregulator for steroid receptor functions. *Mol Endocrinol.* 2005;19:1158-1169.

26. Fuller PJ, Yang J, Young MJ. 30 years of the mineralocorticoid receptor: coregulators as mediators of mineralocorticoid receptor signalling diversity. *J Endocrinol.* 2017;234:T23-T34.

27. Yang J, Fuller PJ, Morgan J, et al. Use of phage display to identify novel mineralocorticoid receptor-interacting proteins. *Mol Endocrinol.* 2014;28:1571-1584.

28. Eide EJ, Vielhaber EL, Hinz WA, Virshup DM. The circadian regulatory proteins BMAL1 and cryptochromes are substrates of casein kinase Iepsilon. *J Biol Chem.* 2002;277:17248-17254.

29. Piwien Pilipuk G, Vinson GP, Gomez Sanchez C, Galigniana MD. Evidence for NL1-independent nuclear translocation of the mineralocorticoid receptor. *Biochemistry.* 2007;46:1389-1397.

30. Yang P, Sale WS. Casein kinase I is anchored on axonemal doublet microtubules and regulates flagellar dynein phosphorylation and activity. *J Biol Chem.* 2000;275:18905-18912.

31. Werner A, Iwasaki S, McGourty CA, et al. Cell-fate determination by ubiquitin-dependent regulation of translation. *Nature.* 2015;525:523-527.

32. Meier UT, Blobel G. A nuclear localization signal binding protein in the nucleolus. *J Cell Biol.* 1990;111:2235-2245.

33. Thomas Meier U, Blobel G. Nopp 140 shuttles on tracks between nucleolus and cytoplasm. *Cell.* 1992;70:127-138.

34. Sakai D, Trainor PA. Face off against ROS: Tcof1/Treacle safeguards neuroepithelial cells and progenitor neural crest cells from oxidative stress during craniofacial development. *Dev Growth Differ.* 2016;58(7):577-585.

35. Gao X, Wang Q, Li W, et al. Identification of nucleolar and coiled-body phosphoprotein 1 (NOLC1) minimal promoter regulated by NF-kB and CREB. *BMB Rep.* 2011;44:70-75.

36. Le Biliari F, Khan JA, Lamribet K, et al. Cistrome of the aldosterone-activated mineralocorticoid receptor in human renal cells. *FASEB J.* 2015;29:3977-3989.

37. Guo Y, Jia P, Chen Y, et al. PHLDA1 is a new therapeutic target of oxidative stress and ischemia reperfusion-induced myocardial injury. *Life Sci.* 2020;245:117347.

38. Han C, Yan P, He T, et al. PHLDA1 promotes microglia-mediated neuroinflammation via regulating K63-linked ubiquitination of TRAF6. *Brain Behav Immun.* 2020;88:640-653.

39. Cegielska A, Gietzen KF, Rivers A, Virshup DM. Autoinhibition of casein kinase I epsilon is relieved by protein phosphatases and limited proteolysis. *J Biol Chem.* 1998;273:1357-1364.

40. Yong TJK, Gan YY, Toh BH, Sentry JW. Human CKI alpha L and CKI alpha S are encoded by both 2.4- and 4.2-kb transcripts, the longer containing multiple RNA-destablising elements. *Biochim Biophys Acta.* 2000;1492:425-433.

41. Zhang P, Bill K, Liu J, et al. MiR-155 is a liposarcoma oncogene that targets casein kinase-1 alpha and enhances beta-catenin signaling. *Cancer Res.* 2012;72(7):1751-1762.

42. Cruciat CM, Dolde C, de Groot RE, et al. RNA helicase DDX3 is a regulatory subunit of casein kinase 1 in Wnt-beta-catenin signaling. *Science.* 2013;339:1436-1441.

SUPPORTING INFORMATION

Additional supporting information may be found in the online version of the article at the publisher's website.